


Article

Bearing Capacity of Forest Roads on Poor-Bearing Road Subgrades following Six Years of Use

Grzegorz Trzciński 

Department of Forest Utilization, Institute of Forest Sciences, Warsaw University of Life Sciences—SGGW, 159 Nowoursynowska St., 02-776 Warsaw, Poland; grzegorz_trzcinski@sggw.edu.pl

Abstract: The research was conducted on a forest road on the territory of the State Forests in Poland, in the Brzeziny Forest District, where eight test sections with a total length of 422 m were created with different pavement system on a low-bearing soil substrate (clay, silt loam) as part of the road reconstruction in 2016. The bearing capacity of the pavement was evaluated based on the static strain modulus M_E $\text{MN}\cdot\text{m}^{-2}$ by measuring with a statistic plate (VSS), the dynamic deformation modulus E_{vd} $\text{MN}\cdot\text{m}^{-2}$ obtained from lightweight deflectometer measurements, and the elastic deflection of the pavement U_s mm evaluated from Benkelaman beam measurements. It has been shown that pavements made of crushed aggregate and common gravel on timber roller substructure maintain good bearing capacity parameters, where the average values of secondary modulus of strain are above $130 \text{ MN}\cdot\text{m}^{-2}$, and in the case of pine rollers, this modulus has increased. Pavements on low-bearing soils reinforced with willow brushwood mattresses have low bearing capacity parameters, with averages of $26.09 \leq M_{EII} \leq 53.93$ and $22.1 \leq E_{vd} \leq 39.1 \text{ MN}\cdot\text{m}^{-2}$, but the technical condition of the pavement makes it possible to continue carrying out forestry-related transportation. The research confirms the possibility of reinforcing soils with poor bearing capacity with wooden rollers, and in the case of willow mats for roads with light truck movements.

Keywords: VSS measurements; lightweight deflectometer E_{vd} ; pavement of road; subgrade reinforced with timber logs; willow brushwood mattresses



Citation: Trzciński, G. Bearing Capacity of Forest Roads on Poor-Bearing Road Subgrades following Six Years of Use. *Forests* **2022**, *13*, 1888. <https://doi.org/10.3390/f13111888>

Academic Editor: Stefano Grigolato

Received: 26 September 2022

Accepted: 8 November 2022

Published: 10 November 2022

Publisher's Note: MDPI stays neutral with regard to jurisdictional claims in published maps and institutional affiliations.



Copyright: © 2022 by the author. Licensee MDPI, Basel, Switzerland. This article is an open access article distributed under the terms and conditions of the Creative Commons Attribution (CC BY) license (<https://creativecommons.org/licenses/by/4.0/>).

1. Introduction

Forest roads ensure the proper functioning of forest management [1,2] with their specific conditions of use, designed in a similar or different way than public roads [3–5].

The construction of forest road surfaces on weak roadbeds requires reinforcement in order to obtain the load-bearing parameters of the entire road structure to allow forestry-related transportation, regardless of weather conditions, especially roundwood transport by heavyweight vehicles [6–9]. This is all the more important when dealing with overloaded round wood transport sets above the permissible gross weight [10–13], or to improve the efficiency of wood transport, increasingly heavier transport sets are allowed [14–16].

Pavement elements are subjected to loads by the movement of vehicle wheels, which induce vertical, horizontal and shear stresses that contribute to the deformation of the road structure [6,7,17–20]. The load-bearing capacity and durability of road structures and pavements are influenced by many factors, among which the most common are the parameters of the materials used, water and moisture conditions of the road body, design solutions and the road bed [3,8,21–24]. Particular attention is paid to the importance of road base parameters on the load-bearing capacity of forest roads [6–8,25,26].

The main aspect described in studies of the technical condition of forest roads is their load-bearing capacity [5–9,25–28], the damage that occurs (ruts, potholes) [3,5] and the parameters of the road body [3,8]. Studies also analyze the effects of aggregate degradation [29] and hydrological occurrences [30], as well as the possibility of using various

measurement methods to assess the technical condition of roads [5,31–33]. Measurements of the technical condition of forest roads often use equipment used in public roads [34–36].

The method of reinforcing road surfaces with wooden rollers or willow brushwood mats was known much earlier than the use of geosynthetics [37,38], and it was also used in the State Forest Districts of Poland's State Forests [39,40]. The variety of solutions used (sometimes incidental) for reinforcing with wooden rollers and willow mats on forest roads in forest districts contributed to the development of construction solutions and the building of experimental sections of forest roads in 2016 [39].

The aim of the study is to confirm the suitability of the applied low-bearing soil reinforcements with wooden rollers and willow mats on forest roads made in 2016. Obtaining positive results of the technical condition of the roads and good load-bearing parameters of the pavement will confirm the possibility of using such road structures on weak road substrates.

The research hypothesis was that the load-bearing capacity and pavement structure of forest roads on low-bearing soils reinforced with wooden rollers or willow brushwood mats would not significantly deteriorate after several years of use, and the condition of the pavement would allow the road to continue to be used for forest management.

The following issues were considered in the study:

- (1) Analysis of pavement bearing capacity under static loading (VSS statistic plate and dynamic plate);
- (2) Analysis of pavement deflections under dynamic loading with a Benkelman beam;
- (3) Analysis of the loading of the road with heavy traffic (round wood transport);
- (4) Comparison of the obtained results with the original data.

2. Materials and Methods

2.1. The Analyzed Section of the Forest Road

The research was conducted on a forest road on the territory of the Polish State Forests in the Brzeziny Forest District, Wiączyń forest complex, along the forest units 164/170 (GPS 51.790048880716434, 19.65544477298789–51.78323823685908, 19.647842602109776). The road is the main route for the entire forest complex with the habitat type of fresh forest, with an area of 975.71 ha covering 39 forest units. The road provides a connection between the national road No. 72 in very close proximity to the A1 highway and junction No. 21 'Brzeziny' and the local road. The area is dominated by deciduous stands (birch—*Betula pendula* L., hornbeam—*Carpinus betulus* L., oak—*Quercus robur* L.) and pine trees over 60 years old and older (even over 100 years old). Research sections with different surface structures were created as part of the 2016 road reconstruction on a 422 m section. Eight test sections were carried out on a road with subsoil on low-bearing soils (clayey dust, clayey sands, clays) classified in the weakest group of bearing capacity of road subsoils.

The proposed road is a single, one-lane road with a width of 3.5 m, in both directions and shoulders.

The road sections were built specifically for the research project funded by the Polish State Forest Service, General Directorate of State Forests in Poland, grant number DGLP ER-0333-1/14. The pavement system was designed using crushed aggregates, 0/31.5 mm grain size and sand–gravel mix on a sub-base reinforced with wood rollers (pine or oak) and willow mats. Different variants of the pavement design of the applied rollers and willow mats with aggregate for the pavement were provided to study the impact on the technical parameters of the road and technological aspects, as shown in Table 1. A reference road section without road base reinforcement (Bzw) was carried out only with the profiling of the existing pavement and a new layer of aggregate (Table 1). We used pine and oak logs, mats made of willow and mats with a reinforced structure (timber poles placed in the middle of the mat) using different aggregates (Figures 1 and 2).

Table 1. Pavement construction in the research sections.

Symbol of Road Section	Chainage of the Road Section	Description of Pavement System *
A1	0 + 010 ÷ 0 + 050	180 mm quarry aggregate 0/31.5 mm, 200 mm drainage layer of coarse sand CSa, subgrade reinforced with oak timber logs ϕ 120 ÷ 180 mm filled with sand
A2	0 + 050 ÷ 0 + 092	200 mm sand–gravel mix 0/31.5 mm, 200 mm drainage layer of coarse sand CSa, subgrade reinforced with oak timber logs ϕ 120 ÷ 180 mm filled with sand
B1	0 + 285 ÷ 0 + 320	180 mm quarry aggregate 0/31.5 mm, 200 mm drainage layer of coarse sand CSa, subgrade reinforced with pine timber logs ϕ 120 ÷ 180 mm filled with sand
B2	0 + 250 ÷ 0 + 285	200 mm sand–gravel mix 0/31.5 mm, 200 mm drainage layer of coarse sand CSa, subgrade reinforced with pine timber logs ϕ 120 ÷ 180 mm filled with sand
C1	0 + 320 ÷ 0 + 350	180 mm quarry aggregate 0/31.5 mm, 120 mm drainage layer of coarse sand CSa, subgrade reinforced with 200 mm thick 2.0 × 2.0 m willow brushwood mattresses
C2	0 + 350 ÷ 0 + 375	180 mm sand–gravel mix 0/31.5 mm, 120 mm drainage layer of coarse sand CSa, Subgrade reinforced with 200 mm thick 2.0 × 2.0 m willow brushwood mattresses strengthened with timber logs
C3	0 + 375 ÷ 400	100 mm sand–gravel mix 0/31.5 mm, 160 mm sand–gravel mix 0/63 mm, 400 g·m ⁻² geotextile, alignment layer 50 mm of sand, subgrade reinforced with 200 mm thick 2.0 × 2.0 m willow brushwood mattresses
Bzw	0 + 092 ÷ 0 + 250	120 mm quarry aggregate 0/31.5 mm, existing pavement profiled and thickened

* Prepared on the basis of the technical design of the reconstruction of the forest road.

According to data from the road manager (State Forest District), only as part of warranty repairs before the end of the three-year warranty period (September 2019), road leveling was performed on the study sections, with the 0 + 092 ÷ 0 + 175 m section without reinforcements (Bzw) of the 0/31.5 mm aggregate brought in, and no road work was performed on the other sections.

Based on data from the State Forest District and consultations with the Forester of the Wiączyń Forestry District, it was evaluated that, on the analyzed section, round wood is transported from forestry units 154–172 of the Wiączyń forest complex. In 2017–2022, a total of 3701 m³ of wood was harvested from the above-mentioned units, which amounts to 617 m³ per year. Assuming an average volume of a single load of about 29.0 m³ of timber [12,41], we obtain a total of almost 128 transports with round wood, and 21 transports per year. The studied road section is characterized by a low traffic load of high-tonnage wood transport sets.

**Figure 1.** Reinforcement of the roadbed in the studied sections—oak and pine logs.



Figure 2. Reinforcement of the roadbed in the studied sections—willow brushwood mattress with and without logs reinforcements built in trial.

2.2. Methods for Determining the Bearing Capacity of Forest Road Surfaces

The ability of the tested pavements to absorb loads from vehicle wheels was evaluated by the static modulus of deformation M_E evaluated by measuring with a VSS $\text{MN}\cdot\text{m}^{-2}$ plate, the dynamic deformation modulus E_{vd} $\text{MN}\cdot\text{m}^{-2}$ obtained from lightweight deflectionometer measurements, and the elastic deflection of the pavement U_s mm evaluated from Benkelaman beam measurements. The compacted state of the pavement was evaluated by the deformation index I_0 (also known as the compaction index).

Measurements in 2016 were performed as part of the acceptance of road works in accordance with the “Technical Specification for the Execution and Acceptance of Works”, the number of repetitions of which was much smaller than those obtained in 2022.

2.2.1. Determination of Static Modulus of Deformation—Measurements with a VSS Plate

The measure of pavement bearing capacity is the M_E strain modulus, defined as the ratio of the unit load increment to the strain increment of the tested surface over a fixed range of unit loads multiplied by the diameter of the loading plate [42]. The determination of the pavement’s modulus of deformation M_E was conducted using a 300 mm diameter VSS plate with settlement measurements at one center point of the plate [43,44] at unit loads up to $0.55 \text{ MN}\cdot\text{m}^{-2}$, and M_E was calculated according to Formula No. 1 for a unit load range of $0.25 \div 0.35 \text{ MN}\cdot\text{m}^{-2}$ [42–46]. Measurements were performed with a VSS plate cooperating with a Benkelman beam with electronic recording of the results, and high-tonnage vehicles were used as counterweights. A load of up to $0.55 \text{ MN}\cdot\text{m}^{-2}$ was assumed, since the entire pavement system was tested, not individual structural layers [9].

$$M_E = \frac{3\Delta p}{4\Delta s} D \quad (1)$$

where: Δp —pressure differential [$\text{MN}\cdot\text{m}^{-2}$], Δs —settlement increment corresponding to the pressure difference [mm], D —plate diameter [mm].

VSS plate loading measurements were taken in duplicate at the same point to determine the magnitude of the primary strain modulus M_{EI} and secondary strain modulus M_{EII} . On each section, at least three primary-load strain measurements and three secondary-load measurements were taken at the points that were tested in 2016 with the VSS plate on the road surface on which the wheels of vehicles moved (left and right ruts), as well as a measurement in the centerline of the road. VSS plate measurements were obtained in two rounds, taking measurements in the wheel tracks of vehicles on the left and right sides of the road (left and right ruts, three measurements each) and a control measurement in the axis of the road. A total of 56 measurements were obtained with the VSS plate and static strain modulus (primary and secondary) was calculated from them.

2.2.2. Determination of Dynamic Modulus of Deformation—Lightweight Deflectometer Measurement

The dynamic modulus of strain was evaluated with a lightweight dynamic plate weighing 10 kg. The measurement starts with a preload, where the load is dropped three times, followed by the actual measurement, where the recording device gives the finished result of the E_{vd} modulus in $\text{MN}\cdot\text{m}^{-2}$. The measurement was made at the same road sections and points (left/right side and road axis) as the VSS plate. At least three proper measurements were taken at each point in each series of measurements [47]. A total of 383 measurements were made with the dynamic plate. The first 45 measurements of determining the dynamic modulus (with the dynamic plate) were carried out by the “Classification and Inspection Road Laboratory” from Łódź (a certified laboratory).

2.2.3. Determination of Elastic Deflection—Benkelman Beam Measurement

The value of elastic deflection U_s [mm] was calculated as the doubled difference between the deflection of the loaded pavement and the deflection after the pavement was fully unloaded [48]. Measurements of the deflection of the pavement, with a Benkelman beam deflectometer, were carried out in accordance with the standard [48] according to the variant I—load at descent, and then the elastic deflection was calculated according to Formula (2).

$$U_s = 2(C_0 - C) \text{ [mm]} \quad (2)$$

where: C_0 —reading under load [mm], C —unloading reading [mm].

Over the entire length of the experimental sections of the forest road, deflection measurements were taken between the twin wheels of the rear axle of the transport vehicle (on the rutted surface of the pavement), with a spacing of 6 m between points so that the truck could drive off to the desired distance according to the standard. From the results obtained, the average elastic deflection for the test section and the reliable deflection will be calculated according to Formula (3) [49].

$$U_m = U_{avg} + 2S_u \text{ [mm]} \quad (3)$$

where: U_m —reliable elastic deflection, U_{avg} —the average elastic deflection for a given homogeneous section, S_u —standard deviation of deflections for homogeneous section.

A total of 287 deflection measurements were taken with a Benkelman beam deflection meter. For each section (depending on the length) there were at least 10 measurements in the wheel tracks on the left and right sides of the road.

2.2.4. Determination of Deformation Index I_0

The deformation index I_0 was calculated as the ratio of the secondary strain modulus to the primary strain modulus according to Formula (4).

$$I_0 = \frac{M_{EII}}{M_{EI}} \quad (4)$$

where: M_{EI} —static primary strain modulus [$\text{MN}\cdot\text{m}^{-2}$], M_{EII} —secondary static modulus of strain [$\text{MN}\cdot\text{m}^{-2}$].

2.3. Analysis of Measurement Results

First, an analysis of the results of measurements obtained in 2022 will be presented. Then, a comparative analysis of the obtained strain modulus and strain rate will be carried out between groups of pavements, as well as between the results obtained in subsequent test periods (after the construction of the sections—measurements from 2016 and now 2022). The secondary modulus of strain evaluated after the second load [42,49,50] was adopted for comparative analyses of the load capacity of the tested pavements. In order to analyze in detail the behavior of the pavement system in each section, the analyses of the results from the measurements in the right and left ruts and the road axis are presented, and the

average values were used for comparison with the 2016 data. Comparative analyses will be performed for the average results (M_E , E_{vd} , I_0 , U_s) of the measurements on a particular section and in a given year. Statistical analyses and characterizations (mean, mean \pm Std. error, mean \pm 1.96·Std. error, outliers) of the results were performed using STATISTICA 12.

3. Results

3.1. Bearing Capacity of the Pavement on the Research Sections from Measurements in 2022

3.1.1. Static Strain Modulus Values from Measurements Taken in 2022

Taking 56 complete deflection measurements with the VSS plate allowed the calculation of primary and secondary modules of deformation according to Formula (1). The obtained values of primary and secondary modules of deformation differ between sections, as well as on the same section, measurement on the right and left side of the road and in the axis (Table 2).

Table 2. Values of static modulus of primary and secondary deformation for the tested pavements.

Section	Road Side	Value of Static Strain Modulus [$\text{MN}\cdot\text{m}^{-2}$]							
		Primary			In the Road Axis	Secondary			
		Mean	Range of Results			Mean	Range of Results		In the Road Axis
		Min.	Max.		Min.	Max.			
A1	Left	95.03	62.50	150.00	39.47	203.53	173.08	250.00	160.71
	Right	48.58	34.62	56.25		135.42	125.00	140.63	
A2	Left	70.95	59.21	83.33	30.41	157.05	125.00	173.08	90.00
	Right	52.83	44.12	60.81		121.50	107.14	132.25	
B1	Left	52.08	46.88	62.50	56.25	144.12	112.50	187.50	132.35
	Right	75.72	70.31	86.54		146.09	118.42	187.50	
B2	Left	77.65	75.00	80.36	60.81	138.54	125.00	150.00	118.42
	Right	75.90	66.18	86.54		145.26	140.63	150.00	
C1	Left	25.95	23.44	28.85	17.44	44.32	38.14	48.91	40.18
	Right	28.02	23.44	32.14		45.06	40.18	50.00	
C2	Left	24.54	24.32	27.44	22.96	47.44	42.45	54.88	56.25
	Right	37.12	30.41	47.87		59.65	53.57	66.18	
C3	Left	23.60	22.50	24.73	16.19	34.52	30.00	39.47	35.71
	Right	20.80	17.31	25.00		37.21	32.14	46.88	
Bzw	Left	69.68	62.50	80.36	72.58	132.52	118.42	160.71	118.42
	Right	65.17	52.33	75.00		141.67	112.50	187.50	

The values of average primary strain modules range from a minimum of $20.80 \text{ MN}\cdot\text{m}^{-2}$ (section C3, right side) to a maximum of $95.03 \text{ MN}\cdot\text{m}^{-2}$ (A1, left side) with a range of all results from $16.19 \text{ MN}\cdot\text{m}^{-2}$ (C3 road centerline) to $150 \text{ MN}\cdot\text{m}^{-2}$ (A1). The smallest differences in primary strain modules values are observed for section B2 and for the given section and between sections C1, C2 and C3.

The average secondary modulus of strain for the tested pavements ranges from a minimum of $34.52 \text{ MN}\cdot\text{m}^{-2}$ (C3 left side) to a maximum of $203.53 \text{ MN}\cdot\text{m}^{-2}$ (A1 left side) with a range of results from $32.14 \text{ MN}\cdot\text{m}^{-2}$ (C3 left side) to $250 \text{ MN}\cdot\text{m}^{-2}$ (A1 left side). The pavement on sections B1 and B2 has good load-bearing capacities with small differences, while on sections A1 and A2, there are good load-bearing capacities but there are differences between measurement points (especially A1 left/right side, and on A2 in the axis of the road). The obtained average secondary modules of $135.42 \div 203.53 \text{ MN}\cdot\text{m}^{-2}$ for roller-

reinforced pavements (sections A1 and A2, and B1 and B2) are satisfactory, and in most of the measurements reached values above $120 \text{ MN}\cdot\text{m}^{-2}$, only the measurement on section B1 with minimum values of $115\text{--}118 \text{ MN}\cdot\text{m}^{-2}$ are slightly smaller. The obtained results of secondary modules for pavement reinforced with willow mats, regardless of the aggregate used and the additional reinforcement of the mats, in the range of $30.00 \div 66.18 \text{ MN}\cdot\text{m}^{-2}$ are low and do not meet the requirements even for light transports (Table 2).

3.1.2. E_{vd} Dynamic Strain Modulus from 2022 Measurements

The values of dynamic modules, like static modules, are different for each research section as well as on the same section but at a different measurement point (picket, left/right side or road axis). The values of the obtained dynamic modules are shown in Table 3, and the statistical characteristics are shown in Figure 3. The largest $75 \text{ MN}\cdot\text{m}^{-2}$ average E_{vd} values were obtained for the A1 section with crushed aggregate pavement on an oak roller substructure, whereas the values for the left and right-side measurements coincide. Similar to static modules, the smallest average E_{vd} values of $19.63\text{--}39.04 \text{ MN}\cdot\text{m}^{-2}$ were achieved for sections with willow mats (C1, C2, C3).

Table 3. E_{vd} $\text{MN}\cdot\text{m}^{-2}$ dynamic strain modules values for the tested pavements.

Section	Values of Dynamic Strain Modules E_{vd} $\text{MN}\cdot\text{m}^{-2}$			
	Road Side	Mean	Range of Results	
			Min.	Max.
A1	Left	75.12	46.90	102.74
	Right	75.68	57.11	99.56
	Road axis	45.94	24.06	68.81
A2	Left	61.48	46.68	72.35
	Right	62.94	54.50	78.40
	Road axis	38.38	31.40	45.64
B1	Left	56.15	41.44	75.50
	Right	68.62	50.20	85.88
	Road axis	36.75	18.91	46.58
B2	Left	59.03	33.33	75.25
	Right	61.73	50.00	76.01
	Road axis	38.35	21.63	52.45
C1	Left	37.36	21.57	47.77
	Right	39.04	26.72	54.61
	Road axis	26.14	19.18	33.65
C2	Left	27.89	15.55	48.00
	Right	31.31	23.27	48.91
	Road axis	24.59	15.69	34.04
C3	Left	19.63	13.98	29.30
	Right	23.04	14.28	38.20
	Road axis	23.21	14.51	35.71
Bzw	Left	42.76	22.27	65.79
	Right	47.29	28.37	81.52
	Road axis	36.00	19.50	68.39

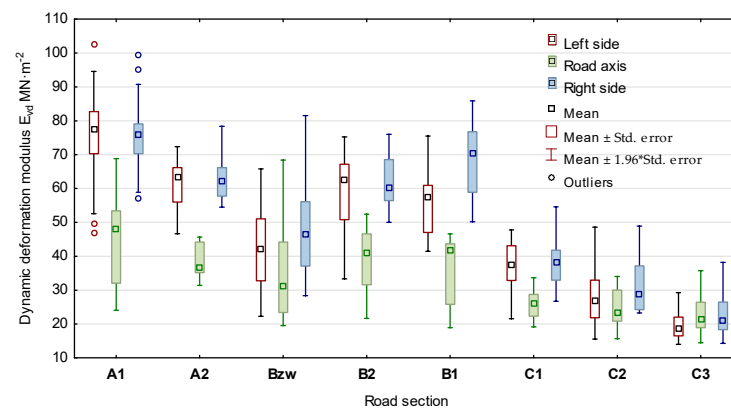


Figure 3. Statistical characteristics of E_{vd} dynamic strain modules from year 2022 measurements.

The value of average dynamic modules E_{vd} in the road axis for most pavements except section C3 is significantly smaller than those obtained in the wheel track (Figure 3).

3.1.3. Analysis of Elastic Deflection and Measured Pavement Deflection

The reliable deflection was then calculated, and a summary of the results for each test section is shown in Table 4. The reference section (Bzw) without reinforcements in the substructure (the longest section) had the most measurements of elastic deflections, with almost identical results for the left and right sides at 1.64–4.50 mm.

Table 4. The values of elastic and measured deflection for the tested pavements.

Section	Road Side	Value of Elastic Deflection [mm]				Number of Measurements
		Mean	Min.	Max.	Reliable	
A1	Left	1.65	1.22	2.12	2.18	16
	Right	1.83	1.20	2.22	2.44	16
A2	Left	2.03	1.54	2.30	2.45	16
	Right	2.43	1.42	3.34	3.52	16
B1	Left	2.27	1.82	3.14	3.07	13
	Right	2.25	1.70	2.76	2.84	13
B2	Left	2.24	1.02	3.12	3.60	13
	Right	2.34	1.58	3.34	3.28	13
C1	Left	2.85	1.98	3.98	4.13	13
	Right	6.19	4.32	7.74	7.90	13
C2	Left	5.97	2.72	8.22	9.43	12
	Right	4.81	3.72	6.22	6.58	12
C3	Left	7.81	6.44	10.68	10.78	11
	Right	7.89	7.36	8.70	8.75	11
Bzw	Left	2.60	1.72	4.50	3.93	44
	Right	2.64	1.64	4.34	3.82	55

The values (mean, min, max.) of the elastic deflections as well as the reliable deflection measured on the right and left sides for the pavement on the timber roller substructure are similar (Figure 4). The values of average elastic deflections on sections A1–B2 are in the range of 1.65–2.43. The reliable deflection calculated for the left and right sides of the road on sections on the substructure of willow mats differ significantly, which indicates a large discrepancy of the results (significant standard deviation) and that with the use of

combined mats (Figure 2), there is uneven settlement of the pavement under load. The pavements on the willow mats substructure have large average elastic deflections in the range of 2.85–7.89 mm and measured deflections of 4.13–10.78 mm.

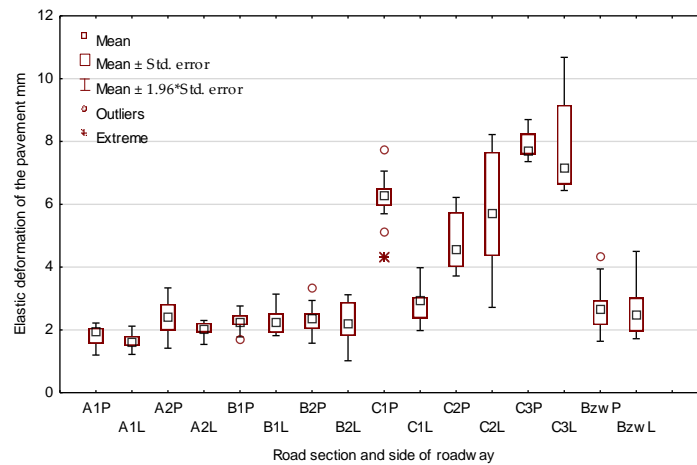


Figure 4. Characteristics of the values of elastic deflections on the tested sections on the left and right sides of the road. (P—right side, L—left side.)

3.2. Pavement Deformation Index I_0

According to the formula for I_0 (Formula (4)), for 56 primary and secondary strain modules of pavements, the strain rate was calculated, and its minimum and maximum values obtained for the test section are shown in Table 5.

Table 5. Pavement deformation index I_0 .

Section	Road Side	Pavement Deformation Index I_0			Road Axis
		Average	Min.	Max.	
A1	Left	2.54	1.25	4.00	4.07
	Right	2.95	2.28	4.06	
A2	Left	2.26	1.78	2.92	2.96
	Right	2.32	2.06	2.47	
B1	Left	2.74	2.40	3.00	2.35
	Right	1.91	1.68	2.17	
B2	Left	1.79	1.61	2.00	1.95
	Right	1.93	1.73	2.13	
C1	Left	1.71	1.59	1.91	2.30
	Right	1.62	1.40	1.76	
C2	Left	1.93	1.85	2.00	2.45
	Right	1.64	1.38	1.79	
C3	Left	1.46	1.33	1.60	2.21
	Right	1.79	1.62	1.88	
Bzw	Left	1.89	1.79	2.00	1.63
	Right	2.16	1.83	2.50	

The obtained minimum values of strain rates of $1.25 \div 2.06$ (for section A1 left side and A2 right side of the road) in most of the pavements, except for section A1 (right side) and B1 measurement on the left side, meet the stipulated condition for I_0 , and the maximum values

of $1.60 \div 4.06$ for the results from measurements on sections A1 and A2 and B1 (left) are higher than acceptable. For 11 cycles of measurements on sections A and B with shafts (road section and measurement point left/right side), I_0 values greater than 2.2 were obtained, with secondary strain modules at good levels on more than one occasion. Good values of I_0 and M_{EII} were obtained for pavements made of interbedded sand (0/31.5 mm) on a pine roller foundation (B2). The pavements reinforced with willow mats are characterized by low strain indices I_0 of $1.33 \div 2.00$ with low values of M_{EII} ($30.00 \div 66.18 \text{ MN}\cdot\text{m}^{-2}$), with the pavements having poor bearing capacity.

3.3. Comparison of Static and Dynamic Strain Modulus Values from 2016 and 2022 Measurements

As already mentioned, there is a very large difference in the number (18/56) of VSS measurements taken (2–3 measurements in 2016, at least 7 per section in 2022) and E_{vd} measurements (14/383), where in 2022 measurements were taken for different points in the cross-section of the roadway (as described above), and in 2016, the location of the measurement (left/right side or axis of the road) was not specified. Average values for the section were taken for comparison and are presented in Table 6.

Table 6. Comparison of static and dynamic strain modulus values from 2016 and 2022 measurements.

Section	Year of Measurement	Value of Static Strain Modulus $\text{MN}\cdot\text{m}^{-2}$			Value of Dynamic Strain Modulus $E_{vd} \text{MN}\cdot\text{m}^{-2}$		
		Mean	Range of Results		Mean	Range of Results	
			Min.	Max.		Min.	Max.
A1	2016	188.81	173.08	104.55	67.97	66.00	69.40
	2022	168.22	125.00	250.00	65.42	24.06	102.74
A2	2016	136.16	107.14	160.71	64.10	-	-
	2022	132.24	107.14	173.08	53.80	31.40	78.40
B1	2016	136.49	132.35	140.63	75.00	-	-
	2022	143.28	112.50	187.50	54.19	18.91	85.88
B2	2016	125.39	118.42	132.35	75.00	74.00	76.00
	2022	138.55	125.00	150.00	52.64	21.63	76.01
C1	2016	50.90	44.12	57.69	39.70	-	-
	2022	44.05	38.14	50.00	34.32	19.18	54.61
C2	2016	48.66	45.00	52.33	38.30	-	-
	2022	53.93	42.45	66.18	27.99	15.55	48.91
C3	2016	26.02	25.57	26.47	22.10	19.20	25.00
	2022	35.84	30.00	46.88	22.43	13.98	38.20
Bzw	2016	141.81	132.35	160.71	77.90	65.00	86.90
	2022	134.42	112.50	187.50	42.01	19.50	81.52

- no range of results (one measurement per test section).

In comparing the values of parameters characterizing the bearing capacity of the pavement between 2016 and 2022, it is important to determine whether the pavement retains its bearing capacity to allow forestry transport despite several years of road use. In four sections (B1, B2, C2 and C3), the average values of secondary modules of strain from the 2022 measurements are higher than in 2016, with a maximum of $13.16 \text{ MN}\cdot\text{m}^{-2}$ for section B2. There is a slight decrease in the average values of secondary modulus of strain in 2022 for the sections on the oak roller substructure (A1 and A2), but many of the results are very good as evidenced by the minimum and maximum values (where the minimum values were most often obtained from measurements in the road axis). The bearing capacity of the pavement in 2022 on section C1 (crushed aggregate on willow mat substructure)

expressed by the secondary modulus of strain is lower compared to 2016, not only the average value, but also over the entire range of results.

The 2022 average values of dynamic modulus of strain E_{vd} $\text{MN}\cdot\text{m}^{-2}$ obtained are lower than in 2016, but this difference is due to the large number of measurements taken also in the road centerline, where there are much lower E_{vd} values (see Table 3 and Figure 3). If one were to compare the average E_{vd} values of 2022 measured in the wheel track (left/right side, Table 3) and the range of results obtained, it could be concluded that pavements on a substructure of wood (oak, pine) rollers maintain E_{vd} values at a satisfactory level. Surfaces on willow mats substructure still (in 2022) have low values of secondary modulus of strain, as well as dynamic modulus of strain.

3.4. Comparison of Deformation Indexes from 2016 and 2022 Measurements

For most sections, the average strain index I_0 obtained in 2022 is smaller than the 2016 measurements, indicating that the pavement (mainly in the wheel tracks) has been compacted by vehicle movements. The maximum values of I_0 were mainly obtained from measurements in the axis of the road.

4. Discussion

The high variability of the obtained results of static deformation modulus (M_{EI} and M_{EII}) from VSS measurements, or dynamic E_{vd} , is pointed out by many authors [8,9,26,51,52]. Direct comparison of parameters characterizing the bearing capacity of the pavement (M_E , E_{vd} results, elastic deflections) made at different times, and this means different weather conditions and, for example, moisture content of the road body, can lead to erroneous conclusions. The results of the obtained modulus from VSS plate and dynamic plate measurements are affected by many factors, and one of the most important is the very way the measurements were obtained [47,51,52]. Research teams presenting the results of forest road bearing capacity measurements with the same equipment and maintaining measurement procedures note the large variance in the results obtained, even on the same research section [8,9,26,53]. Bearing capacity studies of the analyzed sections of the forest road in 2016 were performed with the same VSS plate as in 2022, but with a different counterweight, and dynamic plate studies were performed with different equipment (also in 2022). At the same time, it was not possible to carry out measurements in the same weather conditions as in 2016 (they were not specified, only the known date of the second half of September) as well as in 2022—it was not possible to carry out such a large number of measurements (56-VSS and 383-Evd) with identical conditions (for example, in the measurements in May 2022 there was rainfall). Measurements in 2022 were obtained in the same picket of the road (mileage) at three points (left and right side of the track and axle) as in 2016, in which the exact point of measurement was not recorded. Hence, there may be differences in the results, which is why the comparisons used average values for a given entire road section with a given pavement system.

The obtained average values of secondary modulus of strain (VSS plate test) in 2022 on sections reinforced with wooden rollers (A1, A2, B1 and B2) are satisfactory at a level above $130 \text{ MN}\cdot\text{m}^{-2}$, and in the case of pine rollers (B1 and B2) are higher than in 2016. Assuming that on forest roads there is light or very light traffic (max. KR1), which is also the case on the studied road serving the forest complex (about 30 units), the obtained values of $M_{EII} \geq 120 \text{ MN}\cdot\text{m}^{-2}$ and even in some cases $M_{EII} \geq 140 \text{ MN}\cdot\text{m}^{-2}$ for pavement on wooden rollers ensure the crossing of vehicles with wood.

The observed differences in modulus values from the 2022 measurements between the left and right sides of the road of pavement on wooden rollers may be due to stagnation of water in the ditches on one or the other side of the road, which was observed during the research (Figure A1). For pavement on a willow mats substructure, these differences may be further compounded by the fact that the willow mats were laid in two courses, rather than homogeneously across the entire width of the road (Figure 2).

Aggregate and gravel pavements on a substructure reinforced with willow mats, as in 2016, are characterized by low load-carrying capacity values—static and dynamic modulus (Tables 2 and 3), while the condition of the pavement allows vehicle traffic to proceed except for a section of the end of the test section. This failure may be due to the non-functioning of the drainage in the road, as well as the poor execution of the connection of the further section of the road during its reconstruction (lack of proper alignment of the pavement alignment). It is difficult to assess the suitability of such pavements, with such low bearing capacity parameters $M_{EII} \leq 50 \text{ MN}\cdot\text{m}^{-2}$ and $E_{vd} \leq 40 \text{ MN}\cdot\text{m}^{-2}$ (Tables 2, 3 and 6) and very low traffic of round wood transports, about 21 per year. At the same time, the pavement compaction indices on these sections are at a good level for the most part, $I_0 \leq 2.2$ (Tables 2, 3 and 7).

Table 7. Comparison of deformation indexes from 2016 and 2022 measurements.

Section	Year of Measurement	Deformation Index I_0		
		Mean	Range of Results	
			MIN.	MAX.
A1	2016	2.18	2.00	2.36
	2022	2.94	1.25	4.06
A2	2016	2.42	2.10	2.81
	2022	2.38	1.78	2.96
B1	2016	1.91	1.76	2.06
	2022	2.23	1.68	3.00
B2	2016	2.83	2.76	2.89
	2022	1.87	1.61	2.13
C1	2016	1.90	1.76	2.06
	2022	1.76	1.40	2.30
C2	2016	2.16	2.00	2.32
	2022	1.88	1.38	2.45
C3	2016	1.99	1.85	2.14
	2022	1.71	1.32	2.21
Bzw	2016	2.48	2.14	2.88
	2022	1.97	1.63	2.50

The 200 mm thick willow brushwood mats used are consistent (150–250 mm) with those proposed by Munro [37], but the expected load-bearing parameters were not obtained. Structures on timber rollers (timber grillages) gave positive results and their inherent stiffness can provide better load distribution properties than high strength geotextiles [37]. Willow mats as well as wooden rollers have replaced geosynthetics in the reinforcement of weak road base, so it is worth mentioning here the shortcomings of pavement bearing capacity measurements (VSS plate and light dynamic plate) reported in the literature [54,55]. Obtaining low values of static and dynamic modules on forest roads reinforced with geosynthetics is confirmed, among other studies [8,9,27].

The obtained slightly smaller values of static modules for the sections on oak rollers may additionally result (in addition to the factors affecting the measurement discussed above) also from the behavior (wood decay) of the wooden rollers, although this was not the subject of the current study, but may be illustrated by the acquired slices of rollers from the road sections (Figure A2) [56]. One can see significant biological decomposition of earlywood (sapwood) in oak rollers.

The deformation index I_0 for a properly constructed pavement, depending on the material, should be less than 2.2 and is a measure of pavement compaction, which affects the ability to take loads from vehicle wheels, and its excessive value may be one of the explanations for the causes of rutting. For pavements made of coarse-grained materials (crushed aggregate and aggregate with a grain size of 0/31.5 mm), according to the guidelines of the General Technical Specifications (GTS), the deformation index should be less than 2.2.

5. Conclusions

It has been shown that pavements made of crushed aggregate and common gravel on wooden roller substructure maintain good bearing parameters, where the average values of secondary modulus of strain are above $130 \text{ MN}\cdot\text{m}^{-2}$, and in the case of pine rollers the modulus has increased.

The pavements on low-bearing soils reinforced with willow mats have low bearing capacity parameters, with averages of $26.09 \leq M_{EII} \leq 53.93$ and $22.1 \leq E_{vd} \leq 39.1 \text{ MN}\cdot\text{m}^{-2}$, but the technical condition of the pavements allows further transportation related to forest management. No major damage to the pavement in the form of large ruts is observed.

It seems necessary to increase the thickness of aggregate layers in the pavement to improve its bearing capacity, which also requires further research.

Research confirms the possibility of using the reinforcement of soils with poor bearing capacity with wooden rollers on most forest roads, in particular, in the case of willow mats for forest roads with light truck movement.

Funding: This research was funded by the Polish State Forest Service, General Directorate of State Forests in Poland, grant number DGLP ER-0333-1/14 (construction of sections and implementation of research 2016) and contract order E2271.2.34.2021 (research in 100% and funding in 50% this publication in 2022).

Conflicts of Interest: The authors declare no conflict of interest.

Appendix A



Figure A1. Stagnating water in the ditches of the road during the measurement period in 2022.



Figure A2. Cross-section of pine and oak wood samples taken from rollers from research sections in 2022.

References

1. Coulter, E.D.; Sessions, J.; Wing, M.G. Scheduling forest road maintenance using the analytic hierarchy process and heuristics. *Silva Fenn.* **2006**, *40*, 143–160. [[CrossRef](#)]
2. Paschalis, P. Assumptions to the Rules of Forest Harvest in the Concept of Sustainable and Balanced Forest Management. *Sylvan* **1997**, *14*, 49–56.
3. Aricak, B.; Özer Genç, Ç. Technical Efficiency Evaluation of Forest Roads with Respect to Topo-graphical Factors and Soil Characteristics. *Balt. For.* **2018**, *24*, 123–130.
4. Bruce, J.C.; Han, H.S.; Akay, A.E.; Chung, W. Spreadsheet-Based Cost Estimation for Forest Road Construction. *Western. J. Appl. For.* **2011**, *26*, 189–197. [[CrossRef](#)]
5. Bitir, I.; Derczeni, R.; Lunguleasa, A.; Spirchez, C.; Ciobanu, V. Research on Tracking the Behavior of the Ciobanus Forest Road over a Season Time through Specific Tests and Analysis. *Appl. Sci.* **2022**, *12*, 459. [[CrossRef](#)]
6. O'Mahony, M.J.; Ueberschaer, A.; Owende, P.M.O.; Ward, S.M. Bearing capacity of forest access roads built on peat soils. *J. Terramech.* **2000**, *37*, 127–138. [[CrossRef](#)]
7. Martin, A.M.; Owende, P.M.O.; O'Mahony, M.J.; Ward, S.M. Estimation of the serviceability of forest access roads. *J. For. Eng.* **1999**, *10*, 55–61.
8. Trzciński, G. *Analysis of Technical Parameters of Forest Roads in Terms on Timber Haulage by High-Tonnage Vehicles*; Warsaw University of Life Sciences-SGGW: Warsaw, Poland, 2011; ISBN 978-83-7583-291-1. (In Polish)
9. Czerniak, A.; Grajewski, S.M.; Kurowska, E.E. Bearing Capacity Standards for Forest Roads Constructed Using Various Technologies from Mechanically and Chemically Stabilised Aggregate. *Croat. J. For. Eng.* **2021**, *42*, 477–489. [[CrossRef](#)]
10. McDonnell, K.M.; Devlin, G.J.; Lyons, J.; Russell, F.; Mortimer, D. Assessment of GPS tracking devices and associated software suitable for real time monitoring of timber haulage trucks 2008. In *Annual Report*; COFORD: Ireland, UK, 2008. Available online: <http://www.coford.ie/media/coford/content/publications/projectreports/annualreports/2008-AR-E.pdf> (accessed on 18 February 2022).
11. Hamsley, A.K.; Greene, W.D.; Siry, J.P.; Mendell, B.C. Improving Timber Trucking Performance by Reducing Variability of Log Truck Weights. *South. J. Appl. For.* **2007**, *31*, 12–16. [[CrossRef](#)]
12. Kozakiewicz, P.; Tymendorf, Ł.; Trzciński, G. Importance of the Moisture Content of Large-Sized Scots Pine (*Pinus sylvestris* L.) Roundwood in Its Road Transport. *Forests* **2021**, *12*, 879. [[CrossRef](#)]
13. Moskaliuk, T.; Tymendorf, Ł.; van der Saar, J.; Trzciński, G. Methods of Wood Volume Determining and Its Implications for Forest Transport. *Sensors* **2022**, *22*, 6028. [[CrossRef](#)]
14. Asmoarp, V.; Enström, J.; Bergqvist, M.; von Hofsten, H. Improving Transport Efficiency—Final Report of the ETT 2014–2016 Project. Skogforsk, Arbetsrapport 962-2018. 2018. Available online: <https://www.skogforsk.se/contentassets/d036107f3f2c49ff8d1bfb8d9e122ba1/arbetsrapport-962-2018.pdf> (accessed on 1 July 2022).
15. Palander, T.; Haavikko, H.; Kortelainen, E.; Kärhä, K.; Borz, S.A. Improving Environmental and Energy Efficiency in Wood Transportation for a Carbon-Neutral Forest Industry. *Forests* **2020**, *11*, 1194. [[CrossRef](#)]
16. Liimatainen, H.; Pöllänen, M.; Nykänen, L. Impacts of increasing maximum truck weight—Case Finland. *Eur. Transp. Res. Rev.* **2020**, *12*, 14. [[CrossRef](#)]

17. Lekarp, F.; Isacson, U.; Dawson, A. State of the art. i: Resilient response of unbound aggregates. *J. Transp. Eng.* **2000**, *126*, 66–75. [[CrossRef](#)]
18. Adlinge, S.S.; Gupta, A.K. Pavement Deterioration and its Causes. *J. Mech. Civ. Eng.* **2018**, *10*, 9–15. Available online: [https://www.iosrjournals.org/iosr-jmce/papers/sicete\(civil\)-volume6/60.pdf](https://www.iosrjournals.org/iosr-jmce/papers/sicete(civil)-volume6/60.pdf) (accessed on 18 September 2022).
19. Muttuvelu, D.V.; Kjem, E. A Systematic Review of Permeable Pavements and Their Unbound Material Properties in Comparison to Traditional Subbase Materials. *Infrastructures* **2021**, *6*, 179. [[CrossRef](#)]
20. Varin, P.; Saarenketo, T. Effect of Axle and Tyre Configurations on Pavement Durability—A Prestudy. ROADEX. 2014. Available online: https://www.roadex.org/wp-content/uploads/2014/01/ROADEX_Axle_Tyre_Prestudy_15102014-Final.pdf (accessed on 1 July 2022).
21. Žalimienė, L.; Vaitkus, A.; Čygas, D. Insights and Findings Following 11 Years of Test Road Exploitation. *Coatings* **2020**, *10*, 1161. [[CrossRef](#)]
22. Cetin, A.; Kaya, Z.; Cetin, B.; Aydilek, A.H. Influence of laboratory compaction method on mechanical hydraulic characteristics of unbound granular base materials. *Road Mater. Pavement Des.* **2014**, *15*, 220–235. [[CrossRef](#)]
23. Rahman, S.M.; Erlingsson, S. Influence of Post Compaction on the Moisture Sensitive Resilient Modulus of Unbound Granular Materials. *Int. Conf. Transp. Geotech.* **2016**, *143*, 929–936. [[CrossRef](#)]
24. Akgul, M.; Akburak, S.; Yurtseven, H.; Akay, A.; Cigizoglu, H.; Demir, M.; Ozturk, T.; Eksi, M. Potential impacts of weather and traffic conditions on road surface performance in terms of forest operations continuity. *Appl. Ecol. Environ. Res.* **2019**, *17*, 2533–2550. [[CrossRef](#)]
25. Miler, A.T.; Czerniak, A.; Grajewski, S.; Kamiński, B.; Okoński, B. Marshlands of “LasyRychtalskie” forest promotion complex—Present state and perspective of changes. *Infrastruct. Ecol. Rural. Areas* **2007**, *3*, 21–36. Available online: http://www.infraeco.pl/pl/art/a_15119.htm?plik=289 (accessed on 18 September 2022).
26. Trzciński, G.; Czerniak, A.; Grajewski, S. The functioning of forest communication infrastructure. *Infrastruct. Ecol. Rural. Areas* **2016**, *2*, 527–542. Available online: http://www.infraeco.pl/pl/art/a_17891.htm?plik=1918 (accessed on 18 February 2022).
27. Grajewski, S.M.; Czerniak, A.; Kurowska, E.E. The Influence of Vegetation Succession on Bearing Capacity of Forest Roads Made of Unbound Aggregates. *Forests* **2020**, *11*, 1137. [[CrossRef](#)]
28. Grajewski, S.M. Influence of pavement moisture content on the load-bearing capacity of forest road. *Infrastruct. Ecol. Rural. Areas* **2016**, *IV/2*, 1451–1462. [[CrossRef](#)]
29. De Witt, A.; Boston, K.; Leshchinsky, B. Predicting Aggregate Degradation in Forest Roads in Northwest Oregon. *Forests* **2020**, *11*, 729. [[CrossRef](#)]
30. Kastridis, A. Impact of Forest Roads on Hydrological Processes. *Forests* **2020**, *11*, 1201. [[CrossRef](#)]
31. Waga, K.; Malinen, J.; Tokola, T. A Topographic Wetness Index for Forest Road Quality Assessment: An Application in the Lakeland Region of Finland. *Forests* **2020**, *11*, 1165. [[CrossRef](#)]
32. Girardin, P.; Valeria, O.; Girard, F. Measuring Spatial and Temporal Gravelled Forest Road Degradation in the Boreal Forest. *Remote Sens.* **2022**, *14*, 457. [[CrossRef](#)]
33. Kiss, K.; Malinen, J.; Tokola, T. Comparison of high and low density airborne lidar data for forest road quality assessment. *ISPRS Ann. Photogramm. Remote Sens. Spat. Inf. Sci.* **2016**, *3*, 167–172. [[CrossRef](#)]
34. Kaakkuriavaara, T.; Vuorimies, N.; Kolisoja, P.; Uusitalo, J. Applicability of portable tools in assessing the bearing capacity of forest roads. *Silva Fenn.* **2015**, *49*, 2–25. [[CrossRef](#)]
35. Markó, G.; Primusz, P.; Péterfalvi, J. Measuring the Bearing Capacity of Forest Roads with an Improved Benkelman Beam Apparatus. *Acta Silv. Lign. Hung.* **2013**, *9*, 97–109. [[CrossRef](#)]
36. McFarlane, H.; Paterson, W.; Dohaney, W. *Experience with the Benkelman Beam on Canadian Forest Roads*; Transportation Research Board: Washington, DC, USA, 1975; Volume 16, p. 210.
37. Munro, R. Dealing with Bearing Capacity Problems on Low Volume Roads Constructed on Peat [Online]. ROADEX II Project. Scotland. Available online: http://www.roadex.org/wp-content/uploads/2014/01/2_5-Roads-on-Peat_1.pdf (accessed on 14 December 2019).
38. Godlewski, D. *Nawierzchnie Drogowe. [Pavements of Roads]*; Publishing House of the Warsaw University of Technology: Warsaw, Poland, 2011; ISBN 978-83-7207-965-7. (In Polish)
39. Trzciński, G.; Kozakiewicz, P.; Selwakowski, R. The technical aspects of using timber in the construction of forest roads. *J. Water Land Dev.* **2017**, *34*, 241–247. [[CrossRef](#)]
40. Dzikowski, J.; Szałłowicz, A.; Burzyński, S.; Rajsman, M.; Satoła, J.; Wiązowski, Z. *Drogi Leśne—Poradnik Techniczny*; Ośrodek Rozwojowo-Wdrożeniowy Lasów Państwowych w Bedoniu, DGLP Warszawa-Bedon: Warsaw, Poland.
41. Tymendorf, L.; Trzciński, G. Transport Work for the Supply of Pine Sawlogs to the Sawmill. *Forests* **2020**, *11*, 366. [[CrossRef](#)]
42. *PN-S-02205:1998*; Drogi Samochodowe. Roboty Ziemne. Wymagania i Badania. (Road Car. Earthworks. Requirements and testing). Polish Standard: Warsaw, Poland, 1998.
43. *DIN 18134:2012-04*; Soil—Testing Procedures and Testing Equipment—Plate Load Test. Beuth: Berlin, Germany, 2012. [[CrossRef](#)]
44. *DIN 18134:2001-09*; Determining the Deformation and Strength Characteristics of Soil by The Plate Loading Test. Deutsches Institut für Normung e.V.: Berlin, Germany, 2001.

45. SN 670317b:1998-01; Subgrade. Plate-Loading Test Ev and ME. Swiss Association of Road and Transportation Experts (VSS): Zürich, 1998. Available online: <https://www.mobilityplatform.ch/de/vss-shop/product/670317B> (accessed on 9 November 2022).
46. Węgliński, S. Determination of load action ranges in static and dynamic tests of subgrades by applying rigid plates. *Roads Bridges* **2018**, *17*, 73–88. [[CrossRef](#)]
47. Wyroślak, M.; Ossowski, R. Evaluation of deformation modules in controlled soil embankment based on VSS plate and LFWD plate. *Acta Sci. Pol. Archit.* **2016**, *15*, 111–118. (In Polish)
48. BN-70/8931-06; Drogi Samochodowe. Pomiar Ugięć Nawierzchni Podatnych Ugięciomierzem Belkowym. (Roads Car. Measurement of Deflections of Susceptible Pavements with a Beam Deflection Meter). Polish Standard: Warsaw, Poland, 1978.
49. Lewinowski, C. *Wymiarowanie Podatnych Nawierzchni Drogowych*; (Państwowe Wydawnictwo Naukowe) PWN: Warsaw, Poland, 1980.
50. Rolla, S. *Badania Materiałów i Nawierzchni Drogowych*; (Wydawnictwo Komunikacji i Łączności) WKŁ: Warsaw, Poland, 1985.
51. Krawczyk, B.; Mackiewicz, P.; Szydło, A. Influence analysis of counterweight type used in static plate test on identified parameters of pavement courses and subgrade. *Roads Bridges* **2015**, *14*, 143–157. Available online: <http://www.rabdim.pl/index.php/rb/issue/archive> (accessed on 18 September 2022).
52. Mackiewicz, P.; Krawczyk, B. 2015: Influence of loading time on subgrade parameters derived from VSS static plate test. *Roads Bridges* **2015**, *14*, 19–29. Available online: <https://www.rabdim.pl/index.php/rb/article/view/v14n1p19> (accessed on 18 September 2022).
53. Trzciński, G.; Kaczmarzyk, S. Estimation of carrying capacity of slag and gravel forest road pavements. *Croat. J. For. Eng.* **2006**, *27*, 27–36. Available online: <https://hrcak.srce.hr/file/6552> (accessed on 18 September 2022).
54. Maślakowski, M.; Bartnik, G.; Kowalczyk, S. The influence of geosynthetic reinforcement on choice of the method of subbase deformation measurements. *Bud. Inżynieria Sr.* **2013**, *4*, 281–286. (In Polish)
55. Bartnik, G.; Sulewska, M.J. The use of light weight deflectometer tests for geosynthetics-reinforced soils. *Inżynieria Morska Geotech.* **2015**, *3*, 280–285. (In Polish)
56. Kozakiewicz, P.; Trzciński, G. Wood in the Construction of Forest Roads on Poor-bearing Road Subgrades. *Forests* **2020**, *11*, 138. [[CrossRef](#)]